P2-16

Global migration of ^{13}C impurities in high-density L-mode plasmas in ASDEX Upgrade

A. Hakola[a]*, S. Koivuranta[a], J. Likonen[a], M. Groth[b], T. Kurki-Suonio[b], V. Lindholm[b], J. Miettunen[b], K. Krieger[c], M. Mayer[c], H. W. Müller[c], R. Neu[c], V. Rohde[c], P. Petersson[d], ASDEX Upgrade Team

[a]*VTT, Association EURATOM-Tekes, P.O. Box 1000, 02044 VTT, Finland*

[b]*Aalto University, Association EURATOM-Tekes, P.O. Box 14100, 00076 AALTO, Finland*

[c]*Max-Planck-Institut für Plasmaphysik, EURATOM Association, Boltzmannstr. 2, 85748 Garching, Germany*

[d]*Royal Institute of Technology, Association EURATOM-VR, Teknikringen 31, 10044 Stockholm, Sweden*

Abstract

We have studied the migration of ^{13}C in ASDEX Upgrade after a global impurity injection experiment in 2011. The main chamber was observed to be the largest deposition region for carbon: almost 35% of the injected atoms end up there. Moreover, gaps between wall tiles account for surface densities which are comparable to those on the plasma-facing surfaces. SOLPS modelling of the experiment produced a set of background plasmas and poloidal flow profiles for simulating the transport of ^{13}C with ASCOT; a match with measured deposition, however, required using an imposed flow profile. ASCOT reproduced the observed localized deposition at the outer midplane but work is needed to explain the measured deposition at the inner side of the torus and at the top of the vessel.

PACS: 52.40.Hf, 52.55.Fa, 52.65.Pp, 68.49.Sf

PSI-20 keywords: ASDEX-Upgrade, Edge modelling, Erosion & Deposition, Gas injection & fueling, Surface analysis

**Corresponding author address*: VTT Fusion and Plasma Technology, Association EURATOM-Tekes P. O. Box 1000, 02044 VTT, Finland

**Corresponding author e-mail*: antti.hakola@vtt.fi

Presenting author: Dr. Antti Hakola

Presenting author e-mail: antti.hakola@vtt.fi

1. Introduction

In future fusion devices, the build-up of tritium in plasma-facing components (PFCs) has to be kept at an acceptable level [1,2]. To meet this goal, a thorough understanding of the various fuel-retention mechanisms, including migration of material in the scrape-off layer (SOL) plasma, has to be established.

Experimentally, material migration can be studied by introducing specific impurity atoms in the reactor vessel during a series of identical plasma discharges [3,4]. Among the most suitable impurity isotopes are ^{13}C and ^{15}N: Their natural abundances are small (1.1 at.% for ^{13}C and 0.37 at.% for ^{15}N) and they can be separated from the more common carbon and nitrogen isotopes using standard post mortem surface-analysis techniques.

Here we discuss a global [3] ^{13}C and ^{15}N injection experiment that was carried out in the ASDEX Upgrade (AUG) tokamak in the end of its 2010—2011 experimental campaign. AUG, being a full-W device [5] since 2007, is an ITER-relevant environment for such studies, and so far five global injection experiments have been realized there [4]. In addition to the experiments, attention has been paid to modelling the observed deposition patterns with the ASCOT [6], DIVIMP [7], and SOLPS [8] codes. This article gives an overview of the

2011 experiment and the ^{13}C results as well as the status of the recent modelling efforts with SOLPS and ASCOT. The ^{15}N results will be discussed in [9].

2. Experiments and analyses

2.1 Global ^{13}C and ^{15}N injection experiment in 2011

In the end of the 2010—2011 experimental campaign of AUG, a global ^{13}C and ^{15}N injection experiment was carried out. In the experiment, isotopically labelled methane ($^{13}CH_4$) and nitrogen ($^{15}N_2$) were puffed into the torus during 11 high-density, lower single-null (LSN) L-mode plasma discharges in hydrogen from one valve (in sector 9) at the outer midplane (OMP). The main goal of the experiment was to study the effect of the plasma parameters and the impurity element on the obtained deposition patterns. Another motivation was identifying possible localized deposition hot spots in the AUG torus, guided by the predictions from our previous ASCOT simulations [6].

Altogether 9.2×10^{22} atoms, with 1:1 ratio for ^{13}C and ^{15}N, were puffed into the vessel during the flat-top phases (4.7 s) of the plasma discharges. The relevant AUG shot numbers were #27382—27392 with the following parameters: $n_e=5.8\times10^{19}m^{-3}$($n_e/n_{GW}$~0.57, n_{GW} being the Greenwald density), I_p=0.8MA, B_t=-2.5T, $P_{aux,NBI}$=1.8MW (neutral-beam injection, NBI), and $P_{aux,ECRH}$=0.96MW (electron cyclotron resonance heating, ECRH). The magnetic configuration of the discharge #27385 during its flat-top phase (3-5s) is illustrated in Figure 1. In addition, two set-up shots (#27366 and #27371) with 25-mm strike-point scans and a reciprocating probe measuring electron density and temperature at the OMP were realized.

2.2. Surface analysis of wall tiles

After the injection experiment, 39 standard W-coated wall tiles [5] were removed from different parts of the AUG torus for surface analyses. The poloidal and toroidal locations of the removed tiles, originating from the upper and lower divertor, central heat shield, and two poloidal limiters and ICRH (ion cyclotron resonance heating) antennas A1 and A3 at the

OMP, are highlighted in Figure 1. The antenna A3 and the limiter tile 3 were located on the two sides of the injection valve, while the antennas A1 and limiter tile 2 were toroidally separated from it by -157.5° and +112.5°, respectively. In the outer strike-point region, six special tiles with different marker-stripe configurations had been installed before the 2010—2011 campaign. In this contribution, the results from a marker tile having 3-μm thick poloidal W and W+5%Ta marker stripes on graphite are reported.

The surface density of the deposited ^{13}C on the tiles was determined using secondary ion mass spectrometry (SIMS) at VTT Technical Research Centre of Finland. The analyses were made with a double focusing magnetic sector instrument (VG Ionex IX-70S); The set-up of the analyses can be found in [4]. With the help of a ^{13}C/W calibration sample, the SIMS data were converted into surface densities in at/cm^2. Finally, the amount of ^{13}C deposited on the analysed PFCs before the injection experiment (approximately 1% of the ^{12}C inventory on them) was subtracted from the results.

3. Deposition of ^{13}C in the AUG torus

3.1 Outer midplane

The outer midplane of AUG, especially the tiles surrounding the injection valve, accounts for the largest ^{13}C surface densities after the 2011 experiment. This can be seen in Figure 2, where the average surface densities of ^{13}C on the analyzed A1 and A3 tiles are shown together with toroidal ^{13}C profiles for the two limiter tiles. The surface densities reach values up to 10^{18}—10^{19}at/cm^2, but decrease rapidly to 10^{16}at/cm^2 when moving ~100mm away from the injection valve. Altogether, almost 15% of the injected ^{13}C atoms are estimated to have been accumulated on the different limiter structures at the OMP.

One should note that the analyzed tiles had been inside the torus during several experimental campaigns of AUG and, as a result, showed thick, co-deposited layers on them.

This may have enhanced the deposition of ^{13}C compared to virgin W surfaces, which was the case in AUG during the previous injection experiment in 2007 [4].

Large differences are observed between the ^{13}C levels on the tiles extracted from different ICRH antennas and poloidal limiters. This indicates that the often used assumption of toroidally symmetric deposition [4] in the torus is not valid but a full 3D treatment is required.

3.2 Upper divertor and inner heat shield

The upper divertor is also a strong deposition hot spot for ^{13}C, with the determined surface densities being comparable to those determined for the antenna A1 tiles (10^{16}—10^{17}at/cm^2, see Figure 3(a)). The poloidal deposition profile is relatively uniform, except for a deposition peak close to the corner zone of tiles i1 and a1 and reduced deposition at the central part of tile i1. A plausible explanation can be found from the formation of a secondary X point (see Figure 1) just in front of tile i1 such that the flux surfaces strike the upper divertor in the above-mentioned zones. During the injection experiment in 2007, a similar double-null-like configuration but with the secondary X point behind tile i1 was used [4]. Matching of the 2007 and 2011 profiles in Figure 3(a) was therefore an anticipated result.

Even higher surface densities of ^{13}C, up to 10^{18}at/cm^2 were measured in the central heat-shield region (see Figure 3(b)). This is especially remarkable since the heat shield is known to be a net erosion area [10]. Furthermore, the ^{13}C levels here are 10—1000 times higher than those observed after the 2007 experiment. We think that the differences in the magnetic configuration explain this qualitatively different deposition behavior. It is conceivable that the poloidal flow pattern has changed with the different location for the secondary X point such that a considerable number of the injected ^{13}C atoms have continued their migration towards the inner parts of the torus.

Assuming toroidally symmetric deposition, we obtained that 15% of the injected ^{13}C atoms have ended up in the heat-shield zone and 4% at the upper divertor. In total, the main chamber thus contains 30-35% of the carbon atoms introduced into the torus.

3.3 Lower divertor and tile gaps

In 2011, deposition of ^{13}C in the lower divertor is generally smaller than in the main chamber and to some degree asymmetric between the outer and inner parts – although not so clearly as in 2007 (see Figure 3(c)). Somewhat larger surface densities are observed on tiles 6A and 6B in 2011 than in 2007 – perhaps due to more ^{13}C atoms flowing towards the inner side of the torus from the upper-divertor and heat-shield regions – while in the roof-baffle zone there are hardly any differences between the two experiments.

In the outer divertor, the situation has dramatically changed from 2007 to 2011 such that now the determined ^{13}C inventories are more than 10 times larger. This could again be attributed to the different magnetic configurations of the two experiments: in 2011 a more direct connection was established from the injection valve to the outer strike zone. The tile surfaces being more eroded after the 2010—2011 plasma operations may have also increased the deposition efficiency of ^{13}C. In addition, the surface densities are somewhat larger on the W+Ta marker than on pure W. Most likely this is not due to the substrate material but different toroidal locations of the two markers: the W stripe had been shadowed from direct plasma contact by the neighboring tiles. However, the entire lower divertor is a minor deposition region for main-chamber impurities: of the injected carbon atoms only 1.5% find their way at the inner divertor, 0.3% in the roof-baffle zone, and 0.4% at the outer divertor.

Deposition in gaps between the tiles was surprisingly large: the observed ^{13}C surface densities were on average $\sim 5\times10^{15}$at/cm^2. Figure 3(d) shows the results collected from a number of samples, taken from the side faces of ICRH, upper-divertor, and lower-divertor

tiles. Considering the large area of the gap regions, the total amount of ^{13}C in gaps can be comparable to the values determined for the front surfaces of the tiles.

4. Modelling of the experiment

4.1 Background plasma simulations with SOLPS

Modelling of the 2011 injection experiment was initiated by simulating the background plasma with the 2D plasma fluid code SOLPS. The main aim was to obtain a range of background plasmas for simulations with ASCOT and a prediction for the poloidal flow profile as this has been noticed to have a significant influence on the simulated deposition distribution for ^{13}C [6,7].

In the simulations, a pure hydrogen plasma without methane or nitrogen injection was used for the shot #27385. The simulation of neutrals was handled by the EIRENE 99 code [8]. The anomalous perpendicular diffusion coefficient was $D_{\perp}$=0.3m^2/s, and a relatively sparse grid with a size of 20×50 was used. In the simulations, the upstream electron density at the separatrix, $n_{e,sep}$ was set as a free parameter and varied in the range 0.5—4.0×10^{19}m^{-3}. The experimental data, extracted from Thomson scattering (TS) and reciprocating probe (MEM) measurements at the OMP and from fixed Langmuir probes (LP) in the vicinity of the inner and outer strike points, were taken from the set-up shot #27366.

Both in the case of n_e and T_e, it was possible to obtain a fairly good match to the measured data – but not simultaneously at the OMP and at the divertor targets. The best fit in the case of n_e at the OMP is shown in Figure 4(a), corresponding to $n_{e,sep}$= 2.25×10^{19}m^{-3}. This background plasma was selected to be used in the ASCOT simulations.

The simulations predict rather weak plasma flow in the AUG main chamber and a stagnation point around the OMP. This behaviour can be seen in Figure 4(b), where poloidal flow profiles along flux surfaces from the inner to the outer divertor target, both close to the separatrix and in the far SOL, are shown for the case investigated in part (a). The resulting

profiles were also included in the ASCOT simulations even though they are known to be in contradiction with the strong flows that are generally observed in tokamaks [11].

4.2 Modelling of ^{13}C transport with ASCOT

The transport of the injected ^{13}C was modeled with the 3D Monte Carlo code ASCOT [6] during the discharge #27385. Here the magnetic equilibrium at 2.8s was used together with the SOLPS background plasma. The halo plasma conditions were approximated with exponentially decaying profiles with decay lengths obtained from the measurements at the OMP. The simulations employed the true 3D wall geometry of AUG, see [6] for additional information.

In the simulations, an ensemble of 300,000 $^{13}C^{+}$ test particles was followed until their deposition. The particles were assumed to be uniformly distributed over a cylindrical volume in the SOL of sector 9 (position of the injection valve). The radial extent of the particle cloud was 50 mm from the OMP separatrix towards the outer wall, the diffusion coefficient was $D_{\perp}$=0.25m^2/s, and the initial energy of the particles E_0=0.3eV. A detailed description of the simulation setup and the applied model for the SOL plasma can be found in [6].

ASCOT simulations with the weak SOLPS plasma flows showed very strong ^{13}C deposition (almost 50% of the injected particles) at the outer divertor, in contrast to the experimental results. A better matching divertor asymmetry was achieved by manually imposing a plasma flow of Mach 0.5 towards the divertor targets and with a stagnation point between the outer midplane and the X point, as illustrated in Figure 4(b); for more information on the flows in different regions, see [6]. The deposition pattern calculated with ASCOT using the imposed flow is shown in Figure 4(c) and it indicates that the ^{13}C deposition is the strongest at the inner divertor. Near the injection location, highly localized deposition can be seen on the limiter and ICRH structures. A notable feature is the large

deposition (27%) at the top of the vessel which is due to the double-null magnetic configuration.

5. Conclusions

This article concentrated on the global injection experiment of ^{13}C and ^{15}N in AUG in 2011. Special attention was paid to obtaining a comprehensive set of toroidally and poloidally distributed wall tiles for surface analyses such that the deposition distributions could be studied in detail. Our results showed that the main chamber of AUG is the most prominent sink for carbon in the investigated L-mode discharges: some 35% of the injected atoms had ended up in different regions at the OMP, central heat shield, and the upper divertor. In addition, gaps between tiles are significant deposition regions for ^{13}C. Differences between the deposition profiles in 2007 and 2011 were observed at the heat-shield and outer-divertor regions, and these are expected to be due to the different magnetic configurations and SOL flow profiles of the two experiments. It is also worth noticing that the deposition profiles reported here are different from the long-term ones observed in AUG [4,12]. This could be due to several erosion and re-deposition steps that finally determine the deposition behaviour of carbon.

The SOLPS simulations were able to provide a range of background plasmas and predictions of the poloidal flow profiles. However, ASCOT simulations with the SOLPS solution indicated dominant deposition at the outer divertor, which was not the case experimentally. Therefore, an imposed flow profile was used, and it shifted the strongest deposition peak to the inner divertor, but also predicted localized deposition on the limiter and ICRH structures near the injection location. This shows that the assumption of toroidally symmetric deposition in the torus is not valid as we have also experimentally observed. A notable feature is the prediction of high deposition at the top of the vessel while the observed deposition peak at the heat shield could not be reproduced and the prediction for the

deposition at the inner divertor was far too large. All this we attribute to the effect of the double-null configuration on the poloidal flow, which will be the topic of future studies.

Acknowledgments

This work, supported by the European Communities under the contract of Associations, was carried out within the framework of the European Fusion Development Agreement. The views and opinions expressed herein do not necessarily reflect those of the European Commission.

References

[1] J. Roth et al., Plasma Phys. Control. Fusion 50 (2008) 103001.

[2] J. Roth et al., J. Nucl. Mater. 390—391 (2009) 1.

[3] P. C. Stangeby, J. Nucl. Mater. 415 (2011) S278.

[4] A. Hakola et al., Plasma Phys. Control. Fusion 52 (2010) 065006.

[5] R. Neu et al., Phys. Scr. T138 (2009) 014038.

[6] J. Miettunen et al., Nucl. Fusion 52 (2012) 032001.

[7] T. Makkonen et al., J. Nucl. Mater. 415 (2011) S479.

[8] R. Schneider et al., Contrib. Plasma Phys. 46 (2006) 3.

[9] P. Petersson et al., these proceedings.

[10] K. Krieger et al., J. Nucl. Mater. 307 (2002) 139.

[11] B. Lipschultz et al., Nucl. Fusion 47 (2007) 1189.

[12] M. Mayer et al., J. Nucl. Mater. 390—391 (2009) 538.

Figure captions

Figure 1. Magnetic configuration of the discharge #27385 together with locations of the tiles (in red) removed for surface analyses. The green labels “sec” refer to from which toroidal sector of AUG (out of 16) the tiles originate.

Figure 2. Average surface density of ^{13}C on the studied limiter and ICRH tiles after the 2011 injection experiment.

Figure 3. Poloidal deposition profiles of ^{13}C in the (a) upper divertor (sector 11), (b) central heat shield (sector 12), (c) lower divertor (sector 11), and (d) tile gaps in 2007 and in 2011. The *s* coordinate denotes the poloidal distance along the tile surfaces. Here, ID=inner divertor, OD=outer divertor, and RB=roof baffle. In part (b), the set of data points for each analysed tile correspond to different toroidal locations on them.

Figure 4. (a) Experimental data and the best SOLPS fit for n_e at the OMP. (b) SOLPS predictions for the poloidal flow profile (in Machs) along a flux surface both near the separatrix and in the far SOL and an imposed flow profile used in ASCOT simulations. (c) ASCOT results for the ^{13}C deposition (as percentages of total deposition) in the entire torus using the imposed flow profile. Here, UD=upper divertor.

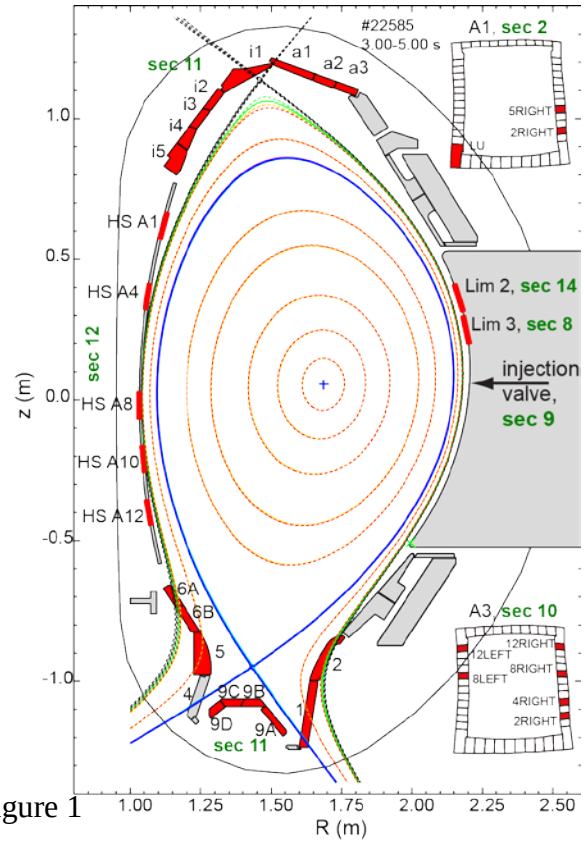
#22585
3.00-5.00 s
A1, sec 2
5RIGHT
2RIGHT
1U
sec 11
i1
a1
a2
a3
i2
i3
i4
i5
HS A1
HS A4
sec 12
HS A8
HS A10
HS A12
Lim 2, sec 14
Lim 3, sec 8
injection
valve,
sec 9
6A
6B
5
4
9C
9B
9D
9A
sec 11
2
1
A3, sec 10
12RIGHT
12LEFT
8RIGHT
8LEFT
4RIGHT
2RIGHT
z (m)
R (m)
1.0
0.5
0.0
-0.5
-1.0
1.00
1.25
1.50
1.75
2.00
2.25
2.50

Figure 1

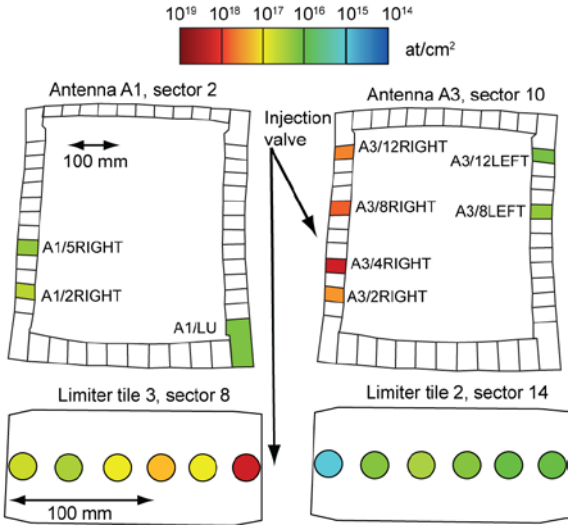
10^19 10^18 10^17 10^16 10^15 10^14
at/cm²
Antenna A1, sector 2
100 mm
A1/5RIGHT
A1/2RIGHT
A1/LU
Injection valve
Antenna A3, sector 10
A3/12RIGHT
A3/12LEFT
A3/8RIGHT
A3/8LEFT
A3/4RIGHT
A3/2RIGHT
Limiter tile 3, sector 8
100 mm
Limiter tile 2, sector 14

Figure 2

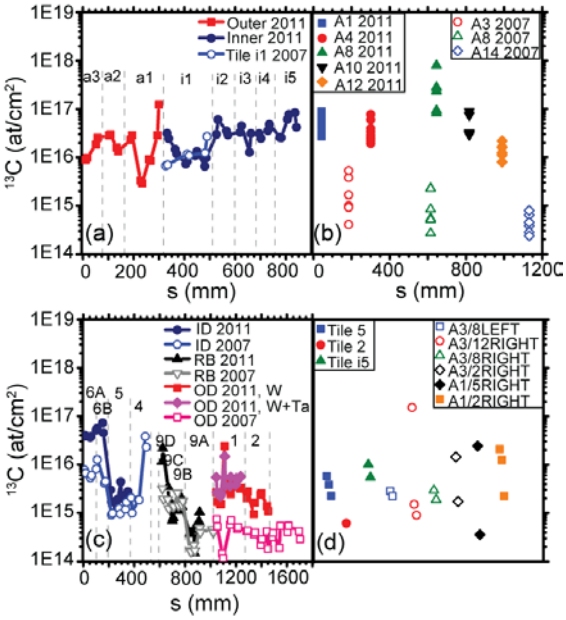
Outer 2011
Inner 2011
Tile i1 2007
a3 a2 a1 i1 i2 i3 i4 i5
(a)
s (mm)
A1 2011
A4 2011
A8 2011
A10 2011
A12 2011
A3 2007
A8 2007
A14 2007
(b)
s (mm)
ID 2011
ID 2007
RB 2011
RB 2007
OD 2011, W
OD 2011, W+Ta
OD 2007
6A 5
6B 4
9D 9A 1 2
9C
9B
(c)
s (mm)
Tile 5
Tile 2
Tile i5
A3/8LEFT
A3/12RIGHT
A3/8RIGHT
A3/2RIGHT
A1/5RIGHT
A1/2RIGHT
(d)
13C (at/cm2)

Figure 3

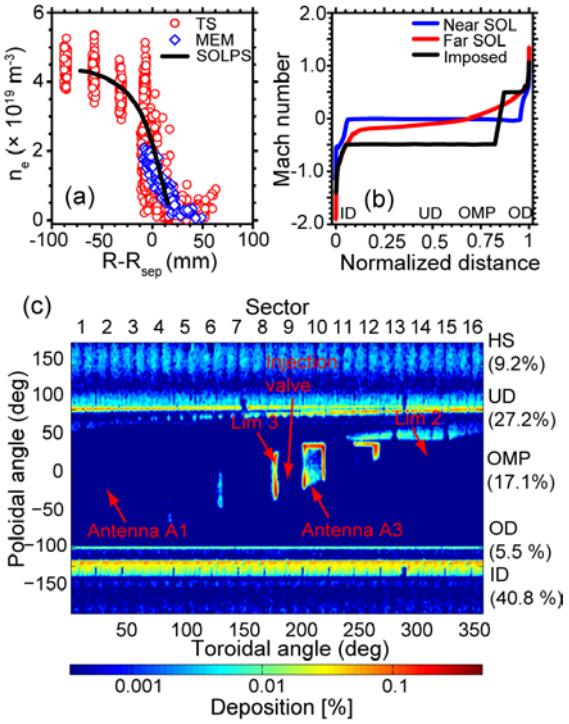
TS
MEM
SOLPS
(a)
n_e (× 10^{19} m^{-3})
R-R_{sep} (mm)
Near SOL
Far SOL
Imposed
Mach number
(b)
ID
UD
OMP
OD
Normalized distance
(c)
Sector
Poloidal angle (deg)
Injection valve
Lim 3
Lim 2
Antenna A1
Antenna A3
HS (9.2%)
UD (27.2%)
OMP (17.1%)
OD (5.5 %)
ID (40.8 %)
Toroidal angle (deg)
Deposition [%]

Figure 4